

# Entropic Plots for Tail Type Classification

Jialin Zhang

Department of Mathematics and Statistics, Mississippi State University  
and

Zhiyi Zhang

Department of Mathematics and Statistics, University of North Carolina  
at Charlotte

April 27, 2022

## Abstract

This article proposes a non-parametric tail classifier to aid tail classification among discrete thick-tail distributions. Theoretical results in this article show that certain distributional tail types can be identified among a sequence of plots based on the tail profile. Such distributional tails include power, sub-exponential, near-exponential, and exponential or thinner decaying tails. The proposed method does not hypothesize the distribution parameters values for classification. The method can be used practically as a preliminary tool to narrow down possible parametric models for refined statistical analysis with the unbiased estimators of the tail profile. Besides, simulation studies suggest that the proposed classification method performs well under various situations.

*Keywords:* discrete tail-classifier, non-parametric statistics, thick tail distributions.

# 1 Introduction and Summary

One of the most basic and acute questions in statistical practice is to determine what parametric model is appropriate for an underlying random variable,  $X$ , in and only in the very distant tail, based on sample data. Such a determination is inherently difficult for at least two reasons. First, the distributional behavior of  $X$  in the tail and that of  $X$  in the rest of the sample space could be qualitatively and vastly different, and therefore it is not clear how the sample data, most of which are observed in the high-frequency region of the sample space, can be suitably used to make the determination. Second, observed data in the tail are perpetually and relatively small in volume (in fact, there may be none) and sparse in coverage. Both of these two reasons directly pertain to the reality that statistical information in a sample, however large, is weak regarding the tail of the underlying distribution. However, inspired by Turing's formula, which remarkably recovers useful tail information from an identically and independently distributed (*iid*) sample, a non-parametric classifier is developed and proposed in this article to aid that determination.

As a motivating example, consider the context of risk management, where it is often of interest to model the distributional tail of the log return of a commodity, say the stock price of Amazon. A fundamental question here is what general class of parametric tail probability models is appropriate for that commodity. Is the Gaussian or exponential tail decay appropriate? Or is the near-exponential, or the sub-exponential, or the power decay more appropriate?

Turing's formula, also known as the Good-Turing formula, was introduced by Good (1953), but largely credited to Alan Turing, to estimate the total probability associated with elements in a discrete sample space that are not represented in an *iid* sample of size  $n$ . Let  $\mathbf{p} = \{p_k; k \geq 1\}$  be a probability distribution on a countably infinite alphabet  $\mathcal{X} = \{\ell_k; k \geq 1\}$ . Let  $\{X_i; i = 1, \dots, n\}$  be an *iid* sample of size  $n$  drawn from  $\mathcal{X}$  under  $\mathbf{p}$ . Let the sample data be summarized into frequencies  $\{Y_k; k \geq 1\}$  and relative frequencies  $\{\hat{p}_k = Y_k/n; k \geq 1\}$ . Further let

$$N_r = \sum_{k \geq 1} 1[Y_k = r] \tag{1}$$

where  $1[\cdot]$  is the indicator function, for  $r = 1, \dots, n$ , and

$$\pi_0 = \sum_{k \geq 1} p_k 1[Y_k = 0], \quad (2)$$

which is the total probability associated with all letters of  $\mathcal{X}$  that are missing in the sample. In the literature,  $\pi_0$  is often referred to as the “missing probability”, and  $1 - \pi_0$  as the “sample coverage of the population” or just simply the “coverage”. Turing’s formula is given by

$$T = \frac{N_1}{n}, \quad (3)$$

whose statistical properties have been studied by many, including most notably Robbins et al. (1968), Esty et al. (1983), Chao et al. (1988), Zhang & Huang (2008), and Zhang & Zhang (2009). For a comprehensive introduction to the subject, interested readers may refer to Zhang (2016).

**Definition 1** (Tail index and tail profile). *Let  $\zeta_v = \sum_{k \geq 1} p_k (1 - p_k)^v$ . Let*

$$\tau_v = v \zeta_v \quad (4)$$

*be referred to as the **tail index**, and  $\{\tau_v; v = v_1, \dots, v_2\}$ , where  $v_1$  and  $v_2$  are two positive integers satisfying  $v_1 < v_2$ , be referred to as a **tail profile**.*

To see that  $\tau_v$  is tail-relevant, it suffices to see that Turing’s formula is tail-relevant. Turing’s formula is related to the tail of a probability distribution in many intricate ways. The first fact to be noted is that Turing’s formula is a good estimator of its estimand,  $\pi_0 = \sum_{k \geq 1} p_k 1[Y_k = 0]$ , a fact proven beyond doubt. Second, it is to be noted that the probabilities,  $p_k$ s, collected in the summation of the estimand,  $\pi_0$ , are likely corresponding to letters with tiny probabilities, and these letters for sufficiently large  $n$  are essentially in the tail, either by common sense or by definition if so chosen. Yet,

$$E(\pi_0) = \sum_{k \geq 1} p_k (1 - p_k)^n = \zeta_n = \tau_n/n.$$

The tail index of (4), or more precisely a profile  $\{\tau_v; v_1 \leq v \leq v_2\}$ , is the base for the tail classifier proposed in this article. What enables the classifier is the existence of an

unbiased estimator of  $\zeta_v$  for every positive integer  $v$ ,  $v \leq n - 1$ , namely

$$Z_v = \frac{n^{v+1}[n - (v + 1)]!}{n!} \sum_{k=1}^{\infty} \left[ \hat{p}_k \prod_{j=0}^{v-1} \left( 1 - \hat{p}_k - \frac{j}{n} \right) \right]. \quad (5)$$

Proposed by Zhang & Zhou (2010),  $Z_v$  is a  $U$ -statistic based on Turing's formula as its kernel function with degree  $v$ , and therefore has many desirable statistical properties. However the most relevant property it has to the issue of this article is the fact that  $E(Z_v) = \zeta_v$  and hence, letting

$$T_v = vZ_v, \quad (6)$$

$E(T_v) = \tau_v$  for  $v \leq n - 1$ . The observed tail profile of interest is

$$\{T_v\} = \{T_v; v = 1, \dots, n - 1\}, \quad (7)$$

which may be viewed as an unbiased estimator of  $\{\tau_v\} = \{\tau_v; v = 1, \dots, n - 1\}$ .

The central idea of the proposed classifier is based on the following Proposition 1, a proof of which is given as a part of the main supportive results in Section 5.

**Proposition 1.** *Let  $\tau_v$  and  $T_v$ , where  $v \leq n - 1$ , be as in (4) and (7) respectively. If  $\tau_v \rightarrow \infty$  as  $v \rightarrow \infty$ , then*

$$\frac{T_v}{\tau_v} \xrightarrow{p} 1. \quad (8)$$

Proposition 1 holds for any general  $\mathbf{p}$  on  $\mathcal{X}$  so long as  $\tau_v \rightarrow \infty$ , which suggests that, when  $\tau_v \rightarrow \infty$ ,  $T_v$  would reasonably capture the increasing trend of  $\tau_v$  in  $v$  for sufficiently large  $v$ .

Zhang (2018) studied the behavior of  $\tau_v$  for different types of  $\mathbf{p}$ , particularly with various tail types, and defined several domains of attraction for all distributions on  $\mathcal{X}$ . Essentially, for distributions with well-behaved tail decays, the property of  $\tau_v \rightarrow \infty$  corresponds to those with thick-tailed distributions. To give a sense for the types of distributions with this property, Zhang (2016) described a sufficient condition for  $\tau_v \rightarrow \infty$ :

**Theorem** (Zhang (2016) Theorem 6.3). *If  $p_{k+1}/p_k \rightarrow 1$ , then  $\tau_v \rightarrow \infty$  as  $v \rightarrow \infty$ .*

This is to say that if  $p_k$  decays slowly then  $\tau_v \rightarrow \infty$ . Examples of distribution satisfying  $p_{k+1}/p_k \rightarrow 1$  include,

$$\text{Power Tail : } p_k \propto \frac{1}{k^\lambda}, \text{ for } k \geq k_0, \text{ where } \lambda > 1 \text{ and } k_0 \geq 1; \quad (9)$$

$$\text{Sub-exponential Tail : } p_k \propto e^{-\lambda k^\alpha}, \text{ for } k \geq k_0, \text{ where } \lambda > 0, \alpha \in (0, 1) \text{ and } k_0 \geq 1; \text{ and} \quad (10)$$

$$\text{Near-exponential Tail : } p_k \propto e^{-\lambda k/(\ln k)^\beta}, \text{ for } k \geq k_0, \text{ where } \lambda > 0, \beta > 0, \text{ and } k_0 \geq 1. \quad (11)$$

The above given distributions have tails decaying with a range of rates, from super slow to almost exponential. They belong to a domain called the Turing-Good family, defined by the property  $\tau_v \rightarrow \infty$  as  $v \rightarrow \infty$ .

Examples of distribution satisfying  $p_{k+1}/p_k \rightarrow c < 1$  include, distributions with exponential tails,  $p_k \propto e^{-\lambda k}$ , for  $k \geq k_0$ , where  $\lambda > 0$  and  $k_0 \geq 1$ ; and distributions with the Gaussian tails,  $p_k \propto e^{-\lambda k^2}$ , for  $k \geq k_0$ , where  $\lambda > 0$  and  $k_0 \geq 1$ . These distributions belong to a domain called the Molchanov family, defined by the property that  $\tau_v$  perpetually oscillates between two positive constants without a limit as  $v \rightarrow \infty$ .

The proposed classifier is, based on an *iid* sample of size  $n$ , to assign the underlying distribution to one of the three thick-tailed sub-domains: power, sub-exponential, or near-exponential. The feasibility of such a classifier is due to the fact that the divergence rates of  $\tau_v$  can be explicitly obtained. It would be shown in the Section 5 that, for sufficiently large  $v$ ,

$$\text{Power Tail Distribution: } \tau_v \asymp v^{1/\lambda}, \quad (12)$$

$$\text{Sub-exponential Tail Distribution: } \tau_v \asymp (\ln v)^{1/\alpha-1}, \quad (13)$$

$$\text{Near-exponential Tail Distribution: } \tau_v \asymp (\ln \ln v)^\beta, \quad (14)$$

where  $\asymp$ <sup>2</sup> represents equality in convergence or divergence rate.

Due to the rates of (12), (13) and (14), if the underlying distribution has one of the tonic forms in (9), (10) or (11), one of the plots of  $(\ln \tau_v \text{ vs. } \ln v)$ ,  $(\ln \tau_v \text{ vs. } \ln \ln v)$ , or  $(\ln \tau_v$

---

<sup>1</sup> $y \propto x$  if  $y = c \cdot x$ , where  $c$  is a constant.

<sup>2</sup> $f(n) \asymp g(n)$  if  $c_1 g(n) \leq f(n) \leq c_2 g(n)$  for sufficiently large  $n$ , where  $c_1$  and  $c_2$  are constants.

vs.  $\ln \ln \ln v$ ) would exhibit a linear trend. Replacing  $\tau_v$  by  $T_v$  for  $v = 3, \dots, n-1$  ( $v$  starts from 3 here because  $\ln \ln \ln 2$  is not a real number), the underlying distribution is classified into the one with the best linear trend. This classifier may be used as a preliminary tool to narrow down possible parametric models for refined statistical analysis.

The rest of the article is organized into several sections. In Section 2, the tail classifier is described in detail, along with a demonstration example. In Section 3, simulation results are presented to evaluate the tail classifier's performance under various distributions and sample sizes. To better understand and use the proposed tail classifier, a few remarks are discussed in Section 4. The supportive theoretical results and proofs are presented in Section 5.

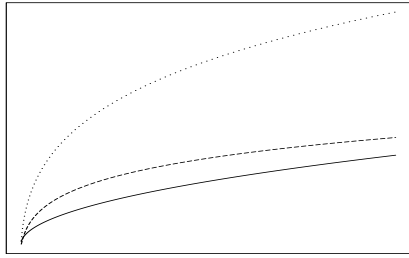
## 2 The Classifier Described

The proposed classifier may be described in terms of four plots, referred to as the entropic plots. They are called entropic plots because the plots are based on  $\{\zeta_v\}$ , also known as entropic moments. Consider the tail profile (see Definition 1), the first plot is  $\tau_v$  versus  $v$ , referred to as Plot I. If the underlying distribution is in one of the three tonic forms in (9), (10) or (11), it can be verified (by the forms in (12), (13) and (14)) that for sufficiently large  $v$ ,

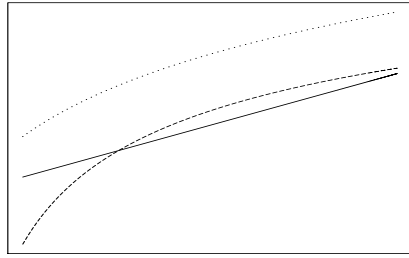
1.  $\tau_v \rightarrow \infty$ , and
2.  $\tau_v$  is a concave function of  $v$ .

These are the two major features of the first plot for a thick-tailed distribution. Figure 1(a) gives the qualitatively typical sketches of  $\tau_v$  for the three tonic forms in (9), (10) or (11) respectively, the solid curve is for power decay, the dashed line is sub-exponential, and the long dashed curve is for near-exponential. It is to be noted that all three curves exhibit the two characteristics mentioned above.

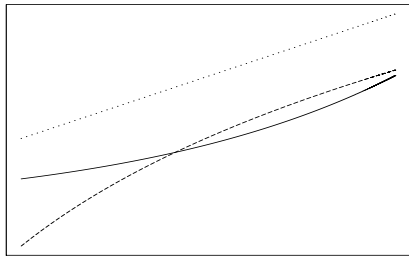
If the tail of the underlying distribution is of form  $p_k \propto e^{-\lambda x}$  or thinner, then  $\tau_v$  oscillates as  $v \rightarrow \infty$  without a limit. This feature suggests that, if  $v$  and the range of the plot,  $(v_1, v_2)$ , are both sufficiently large, then the profile  $\{\tau_v\}$  will exhibit a downturn somewhere in the



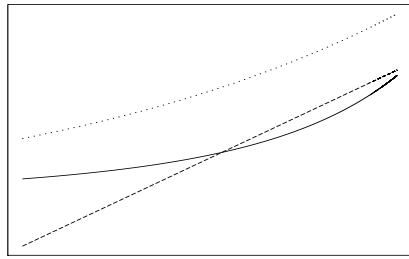
(a)  $\tau_v$  vs.  $v$



(b)  $\ln(\tau_v)$  vs.  $\ln(v)$



(c)  $\ln(\tau_v)$  vs.  $\ln \ln(v)$



(d)  $\ln(\tau_v)$  vs.  $\ln \ln \ln(v)$

Figure 1: Entropic Plots

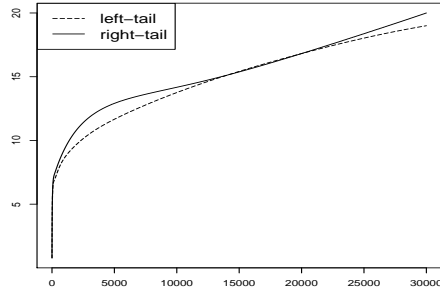
range. An observed downturn would suggest that the tail is very thin, possibly exponential or thinner. This feature will be utilized below to identify distributions with exponential or thinner tails.

The next three plots, referred to as Plots II, III, and IV, are  $\ln \tau_v$  versus  $\ln v$ ,  $\ln \ln v$  and  $\ln \ln \ln v$ , respectively. If the underlying distribution has one of the three tonic tail forms, then one, and only one, of the three curves exhibits the strongest linearity for sufficiently large  $v$ . These features are qualitatively demonstrated in Figures 1(b), 1(c) and 1(d).

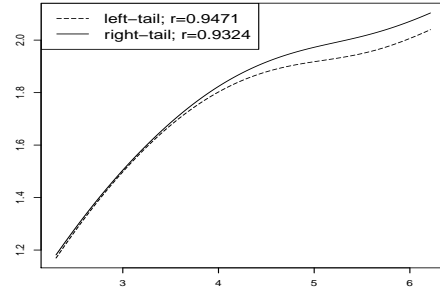
In practice,  $\{\tau_v\}$  is not observed, but  $\{T_v\}$  is. The sample counterparts of those in Figure 1 are plots with (a)  $T_v$  versus  $v$ , (b)  $\ln T_v$  versus  $\ln v$ , (c)  $\ln T_v$  versus  $\ln \ln v$  and (d)  $\ln T_v$  versus  $\ln \ln \ln v$ , respectively.

The steps to carry out the classifier are described and illustrated below with an example

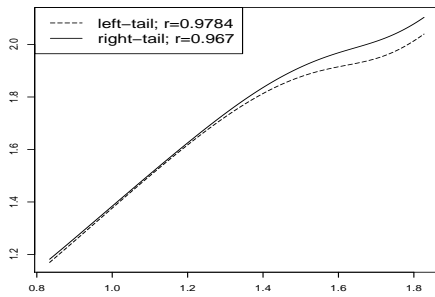
of the log-returns based on the closing minute stock prices of Amazon.com, Inc. (stock symbol AMZN) with a certain discretization. Suppose it is of interest to classify the types of both left-tail and the right-tail of the underlying distribution.



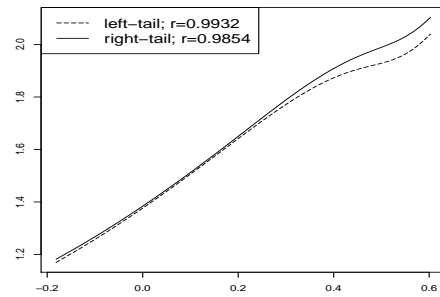
(a)  $T_v$  vs.  $v$ : left-tail and right-tail



(b)  $\ln(T_v)$  vs.  $\ln(v)$ : left-tail and right-tail



(c)  $\ln(T_v)$  vs.  $\ln \ln(v)$ : left-tail and right-tail



(d)  $\ln(T_v)$  vs.  $\ln \ln \ln(v)$ : left-tail and right-tail

Figure 2: Entropic Plots for AMZN

1. Obtain an *iid* sample of size  $n$  and fix a range of index profile from  $v_1$  to  $v_2$ ,  $v_1 < v_2 < n$ . For the AMZN data, let the sample of  $n = 30000$  minute log returns, from 09:31 03/13/2007 to 15:56 06/29/2007, be the base of analysis, and set  $v_1 = 10$  and  $v_2 = 500$ . For an explanation on the choice of tail profile, please refer to discussion under Remark 1 in Section 4.
2. Obtain the sample relative frequencies,  $\{\hat{p}_k\}$  and calculate the observed profile,  $\{T_1, \dots, T_{n-1}\}$ , and plot it against  $v$ ,  $v = 1, \dots, n - 1$ . This step may require a



discretization of the range of the underlying random element. A general rule to follow is that the resulting discretization would support many occupied bins. For the AMZN minute log-returns, the data are processed in two ways. For the right-tail, all the negative observations are aggregated into a single class; and from zero to positive infinity, intervals of the form  $[k\delta, (k + 1)\delta)$  for  $k = 0, 1, \dots$ , where  $\delta = 10^{-4}$ . For the left-tail, all the positive observations are aggregated into a single class; and from zero to negative infinity, intervals of the form  $[-(k + 1)\delta, -k\delta)$  are used. The resulting plots of  $T_v$  versus  $v$  are given in Figure 2 (a), with the solid curve for the right-tail and the long dashed curve for the left-tail.

3. In Figure 2(a), one inspects the trends for large values of  $v$  and looks for a monotonically increasing curve. For sufficiently large  $v$ , the faster the increase, the thicker the tail is. If a flat curve is detected, the distribution is classified as an exponentially decaying tail or thinner. A flat curve is detected if  $\tau_v \rightarrow \infty$ . Flat curves examples are presented in Figure 3. For the AMZN minute log-returns, both tail curves are monotonically increasing, indicating a thick-tailed distribution on both sides.
4. If a classification is not reached in the previous step, then the three other plots are generated, (a)  $\ln T_v$  versus  $\ln v$ , (b)  $\ln T_v$  versus  $\ln \ln v$  and (c)  $\ln T_v$  versus  $\ln \ln \ln v$ . In these three plots, one looks for the strongest linearity. If it is detected in (a), the tail is classified to the power family; if it is detected in (b), the tail is classified to the sub-exponential family; and if it is detected in (c), the tail is classified to the near-exponential family. The strongest linearity is not always easily detected visually. One, however, may calculate the coefficient of correlation,  $r$ , for each plot. The plot with the highest value of  $r$  indicates the strongest linearity and hence prompts a classification. For the AMZN minute log returns, the corresponding plots are presented in Figure 2(b), (c) and (d). The long dashed curves and solid curves all appear to be close to a straight line. However the strongest linearity are both detected in Figure 2(d) indicated by  $r = 0.9854$  and  $r = 0.9932$  respectively, and hence both tails are classified to be a member of the near-exponential family. In fact, since the slopes of the straight lines in Figure 2(d) are approximately  $\hat{m}_{left} = 1.109765$

and  $\hat{m}_{right} = 1.175536$ , a reasonable estimate for  $\beta$ -s are  $\hat{\beta}_{left} = 1.109765$  and  $\hat{\beta}_{right} = 1.175536$  (per (14),  $\ln \tau_v \asymp \beta \cdot \ln \ln \ln v$ ).

### 3 Simulation Results

In this section, simulation results are presented to evaluate the performance of the proposed tail classifier. In this simulation study, four distributions are defined:

Distribution 1 (Power Tail):  $p_v = \frac{6v^{-2}}{\pi^2}, v = 1, 2, 3, \dots$

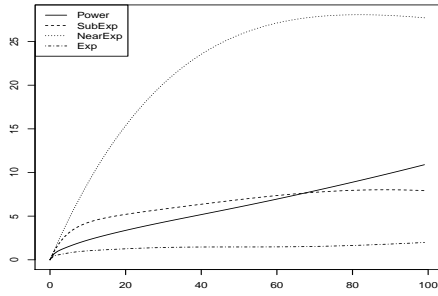
Distribution 2 (Sub-exponential Tail):  $p_v = c_1 \exp(-\sqrt{v})$ , where  $c_1 \approx 0.5986565, v = 1, 2, 3, \dots$

Distribution 3 (Near-exponential Tail):  $p_v = c_2 \exp(-\frac{v+1}{\ln^2(v+1)})$ , where  $c_2 \approx 0.1755221, v = 1, 2, 3, \dots$

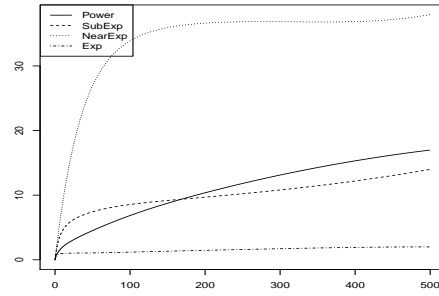
Distribution 4 (Exponential Tail):  $p_v = (e - 1) \exp(-v)$ , where  $e = 2.71828 \dots, v = 1, 2, 3, \dots$

The results are provided in two parts.

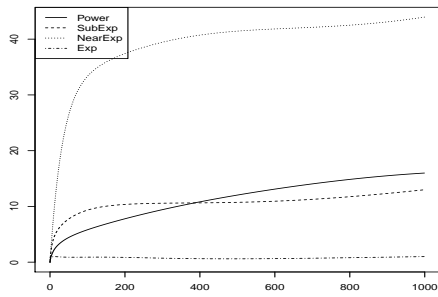
The first part of the simulation results includes six Plot I-s with various sample sizes as shown in Figure 3 to demonstrate the curves of  $T_v$  vs.  $v$ , particularly of those generated under an exponential distribution. In these plots, one observes that only the curves from samples generated under Distribution 4 are flat from the very beginning. Therefore Plot I is sufficient to identify exponential or thinner tails.



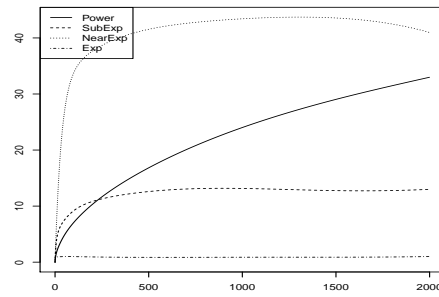
(a)  $T_v$  vs.  $v$ :  $N=100$



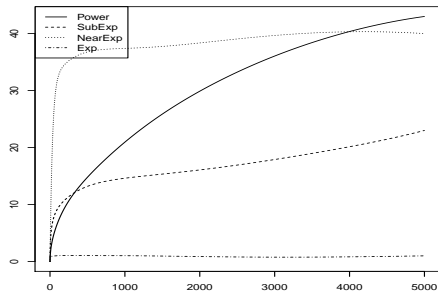
(b)  $T_v$  vs.  $v$ :  $N=500$



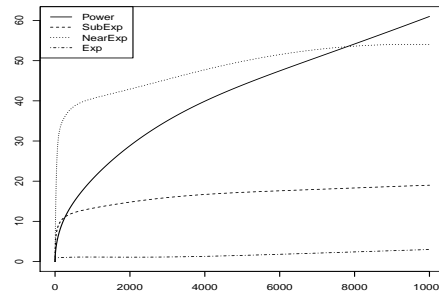
(c)  $T_v$  vs.  $v$ :  $N=1000$



(d)  $T_v$  vs.  $v$ :  $N=2000$



(e)  $T_v$  vs.  $v$ :  $N=5000$



(f)  $T_v$  vs.  $v$ :  $N=10000$

Figure 3: Plot I-s. Only the curves from samples generated under Distribution 4 (Exp) are flat from the very beginning.

In the second part, samples with size  $n = \{100, 500, 1000, 2000, 5000, 10000\}$  are generated under Distributions 1,2, and 3. For each sample size setting, 10000 random samples

were generated. For  $n < 2000$ , the tail profiles were chosen as  $v_1 = 6$  and  $v_2 = 99$ . For  $n \geq 2000$ , the tail profiles were chosen as  $v_1 = 6$  and  $v_2 = n/20$ . The results are summarized in the following Table 1.

n	1→1	1→2	1→3	2→1	2→2	2→3	3→1	3→2	3→3
100	5942	2354	1704	3177	2275	4548	3	3338	6699
500	7747	2246	7	411	6397	3192	0	428	9572
1000	8751	1249	0	69	7454	2477	0	38	9962
2000	9564	436	0	2	8428	1570	0	1	9999
5000	9998	2	0	0	8789	1211	0	0	10000
10000	10000	0	0	0	9040	960	0	0	10000

Table 1: Simulation Results. For example, when  $n = 5000$  and when the samples were generated under Distribution 1, 9998 out of the 10000 random samples were correctly classified as Distribution 1 (hence denoted as 1→1), the remaining two samples were wrongly classified as Distribution 2 (hence denoted as 1→2). For another example, when  $n = 10000$  under Distribution 2, 9040 samples were correctly classified as Distribution 2 (2→2), whereas 960 samples were wrongly classified as Distribution 3 (2→3).

The simulation results show that the proposed classification method’s accuracy is high, particularly when the sample is large. For  $n \geq 2000$ , the simulation results are presented in another perspective in Table 2.

n	$P(1  \rightarrow 1)$	$P(1^C  \rightarrow 1)$	$P(2  \rightarrow 2)$	$P(2^C  \rightarrow 2)$	$P(3  \rightarrow 3)$	$P(3^C  \rightarrow 3)$
2000	0.9998	0.0002	0.9507	0.0493	0.8643	0.1357
5000	1	0	0.9998	0.0002	0.8920	0.1080
10000	1	0	1	0	0.9124	0.0876

Table 2: Simulation Results Represented. “ $i| \rightarrow i$ ” stands for “a sample belongs to Distribution  $i$  given it has been classified as Distribution  $i$ ”, and “ $i^C| \rightarrow i$ ” stands for “a sample does not belong to Distribution  $i$  given it has been classified as Distribution  $i$ ”. The higher the  $P(i| \rightarrow i)$ , the higher the accuracy.

## 4 Miscellaneous

The use of the proposed tail-classification method is further clarified with the following remarks.

**Remark 1.** *The proposed tail classification method is powerful when the sample size is large, and the tail profile is appropriately selected. In practice, only the early stage of the tail profile should be selected unless the sample size is extremely large. Using the latter stage tail profile could lead to unreliable conclusions.*

Take power distributional tail as an example. Theoretically,  $\ln \tau_v \asymp (1/\lambda) \ln v$ , the larger the  $v$ , the better the linearity between  $\ln(\tau_v)$  and  $\ln(v)$  (for simplicity, name this case SL). Practically, there are three barriers against selecting large  $v$ -s.

First, when  $v$  is large, the linearity between  $\ln(\tau_v)$  and  $\ln \ln(v)$  (for simplicity, name this case DL), and between  $\ln(\tau_v)$  and  $\ln \ln \ln(v)$  (for simplicity, name this case TL) are also “quite good”, albeit neither of them have asymptotic linearity according to the theoretical proofs. For example, with the setting Distribution 1 in Section 3, for the profile between 5000 and 8000, measured with  $\rho$ ,  $\rho_{DL} > 0.99997$  and  $\rho_{TL} > 0.99994$ , while the  $\rho_{SL} > 0.9999999999$ . The linearity for DL and TL is “good” because the curvature is not obvious within the large- $v$ -portion of the tail profile, despite  $\ln \tau_v \rightarrow \infty$ . One can observe this phenomenon in Figure 4. Although the linearity between  $\ln(\tau_v)$  and  $\ln(v)$  is indeed the best, it is difficult for  $r(i.e., \hat{\rho})$  to make a correct classification from this part of tail profile. As a consequence, selecting a tail profile with large  $v$  makes the tail-classification inaccurate. Figure 5 offers another view on the tail profile for  $v$  from 10 to 500. Within this tail profile, although the linearity for SL is imperfect yet ( $\rho = 0.999989$ ), its advantage over case DL ( $\rho = 0.9927$ ) and TL ( $\rho = 0.9753$ ) are more significant when comparing with the tail profile in Figure 4. Therefore, for the best classification result, one should adopt the early stage in tail profile for the best distinction. As supplementary examples, similar comparisons with Distribution 2 and 3 are also presented in Figure 6, Figure 7, Figure 8 and Figure 9.

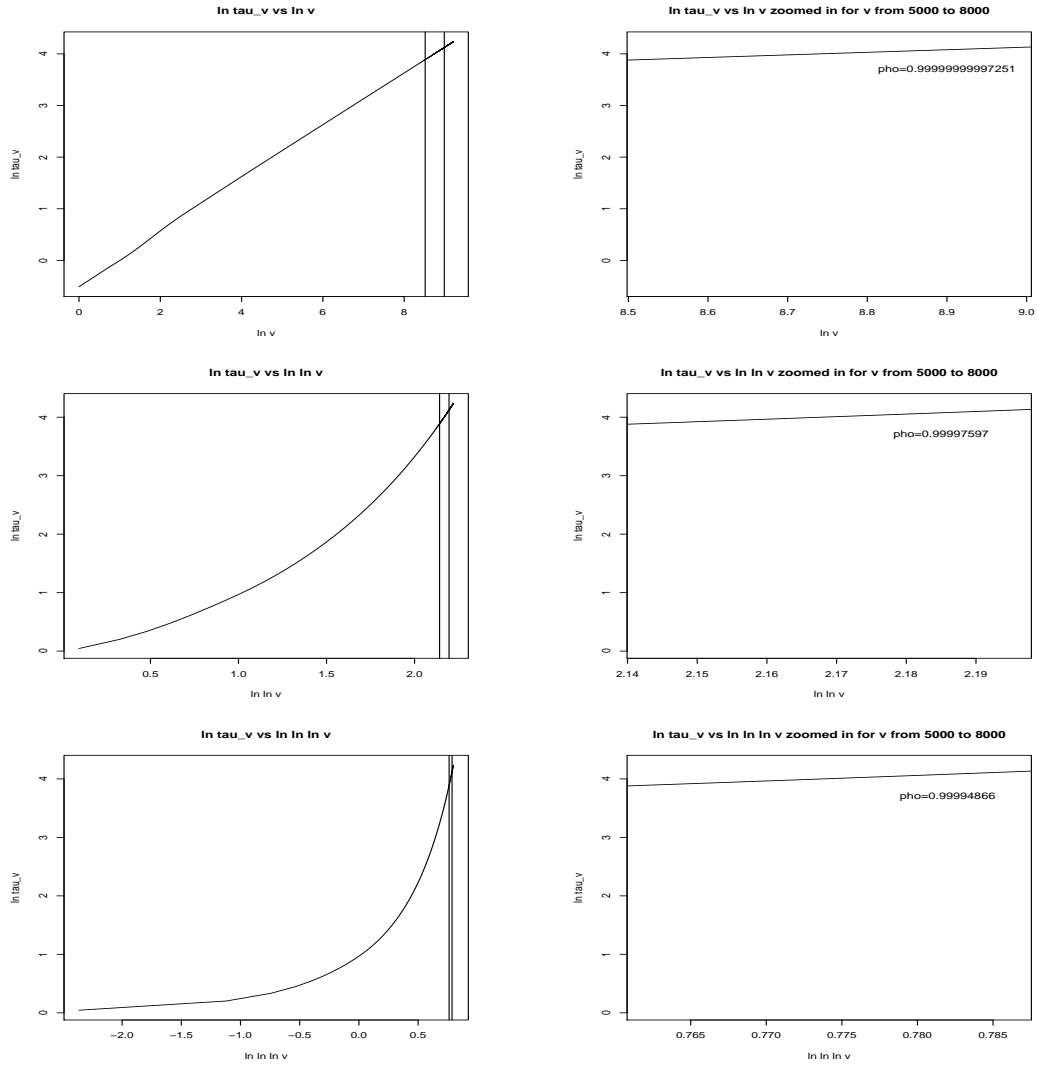


Figure 4: Plots under Distribution 1. Plots on the right side are zoomed for the corresponding part enclosed by two vertical lines on the left-side plots. One observes that although the  $\rho$  in the top right plot is the highest, the two  $\rho$ -s on the other right-side plots are also quite close.

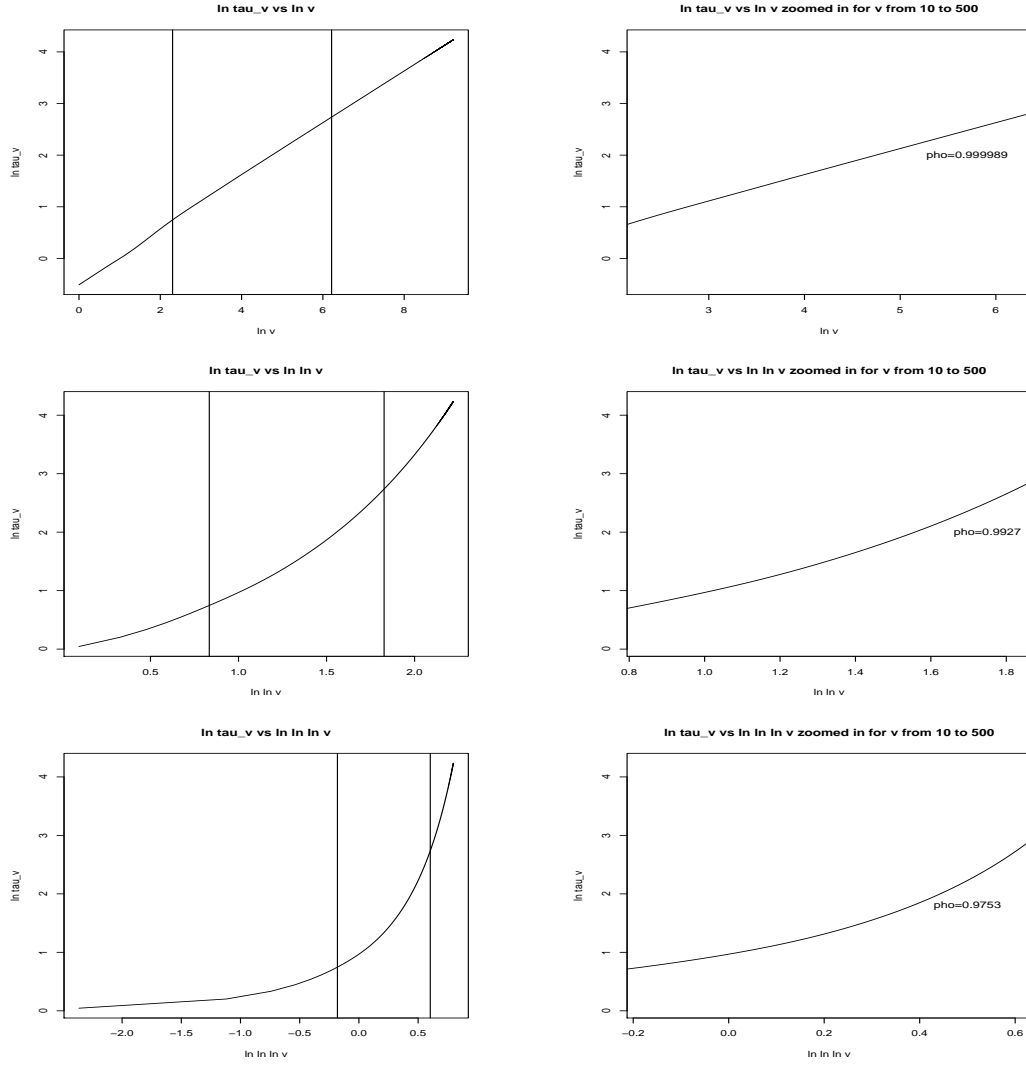


Figure 5: Plots under Distribution 1. Plots on the right side are zoomed for the corresponding part enclosed by two vertical lines on the left-side plots. One observes that although the  $\rho$  in the top right plot not as high as the corresponding  $\rho$  in Figure 4, its advantages over the two  $\rho$ -s on the other right-side plots are much larger compare to that in Figure 4.

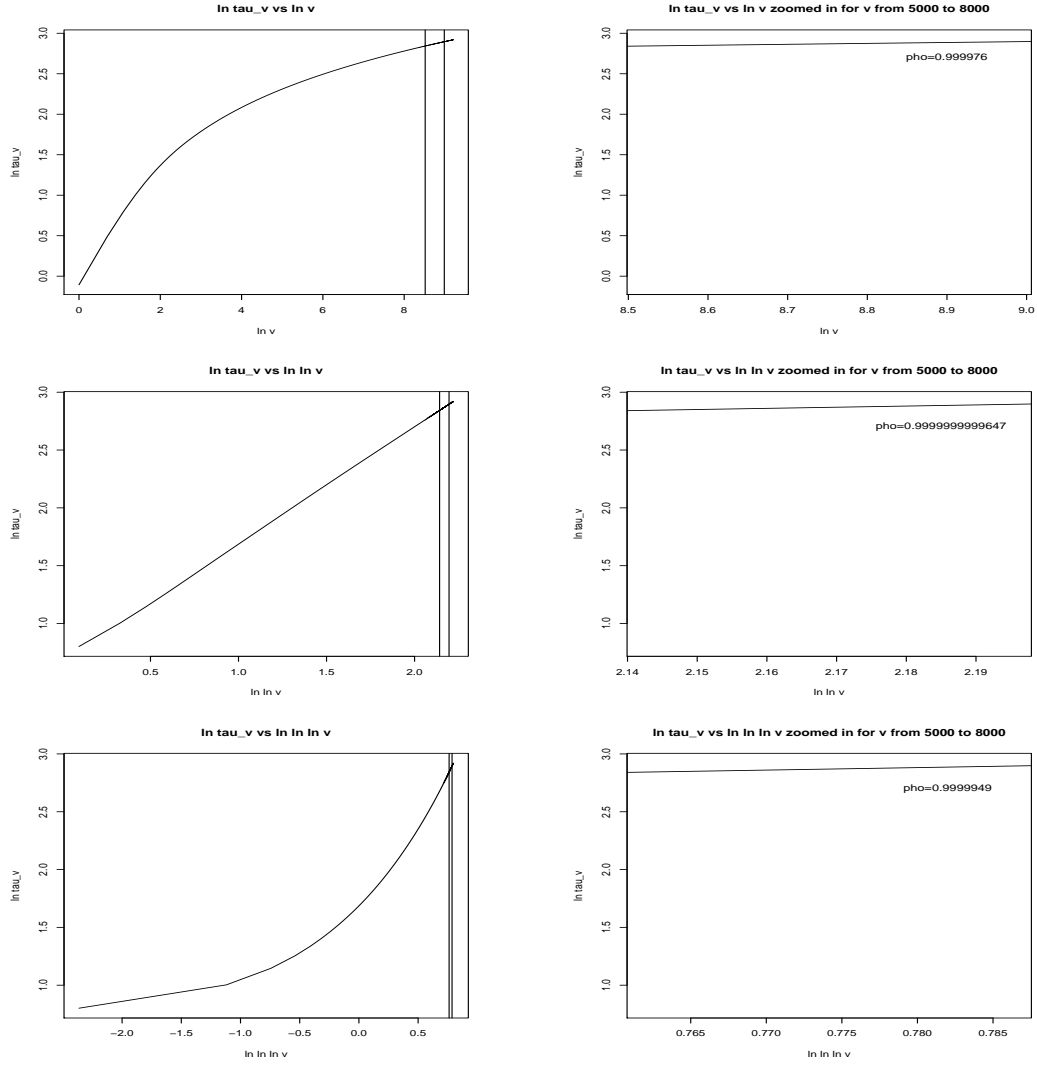


Figure 6: Plots under Distribution 2. Plots on the right side are zoomed for the corresponding part enclosed by two vertical lines on the left-side plots. One observes that although the  $\rho$  in the middle right plot is the highest, the two  $\rho$ -s on the other right-side plots are also quite close.



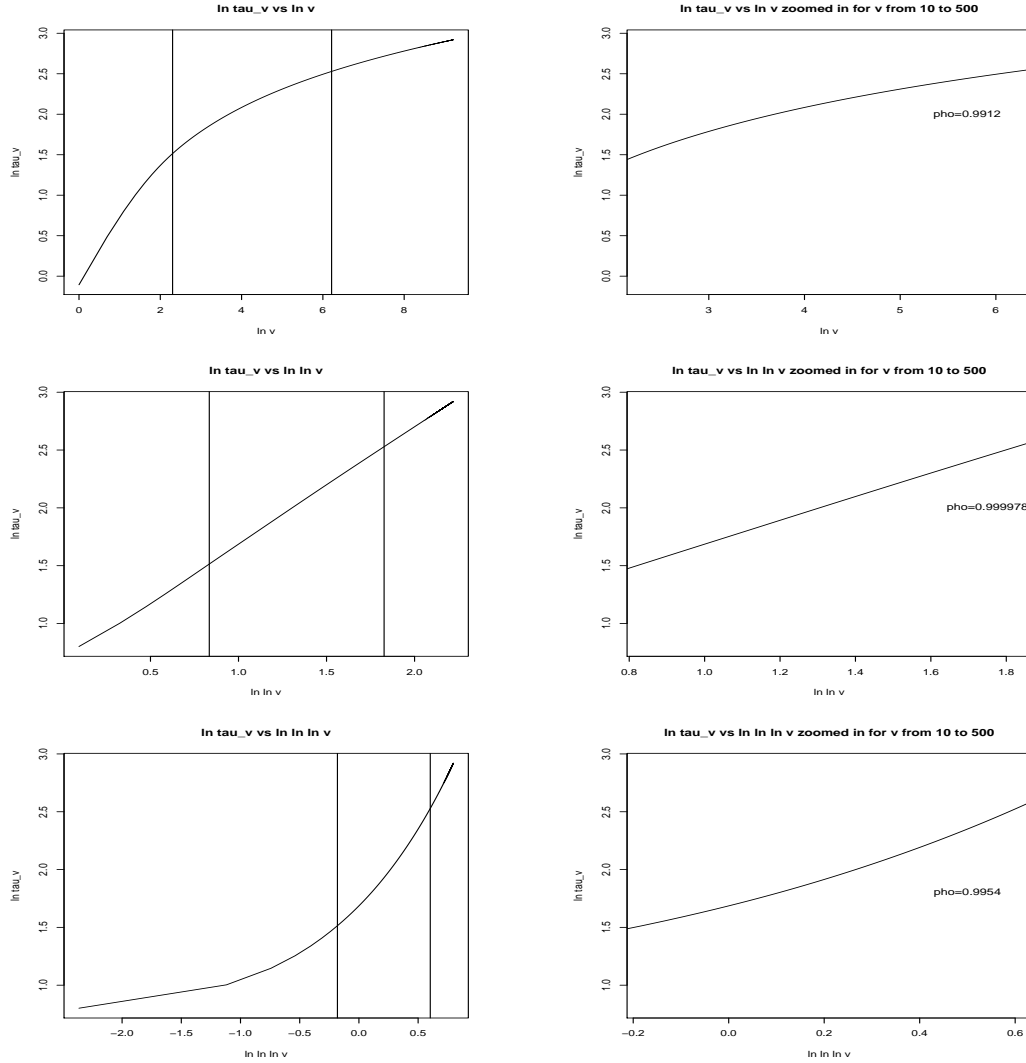


Figure 7: Plots under Distribution 2. Plots on the right side are zoomed for the corresponding part enclosed by two vertical lines on the left-side plots. One observes that although the  $\rho$  in the middle right plot not as high as the corresponding  $\rho$  in Figure 6, its advantages over the two  $\rho$ -s on the other right-side plots are much larger compare to that in Figure 6.

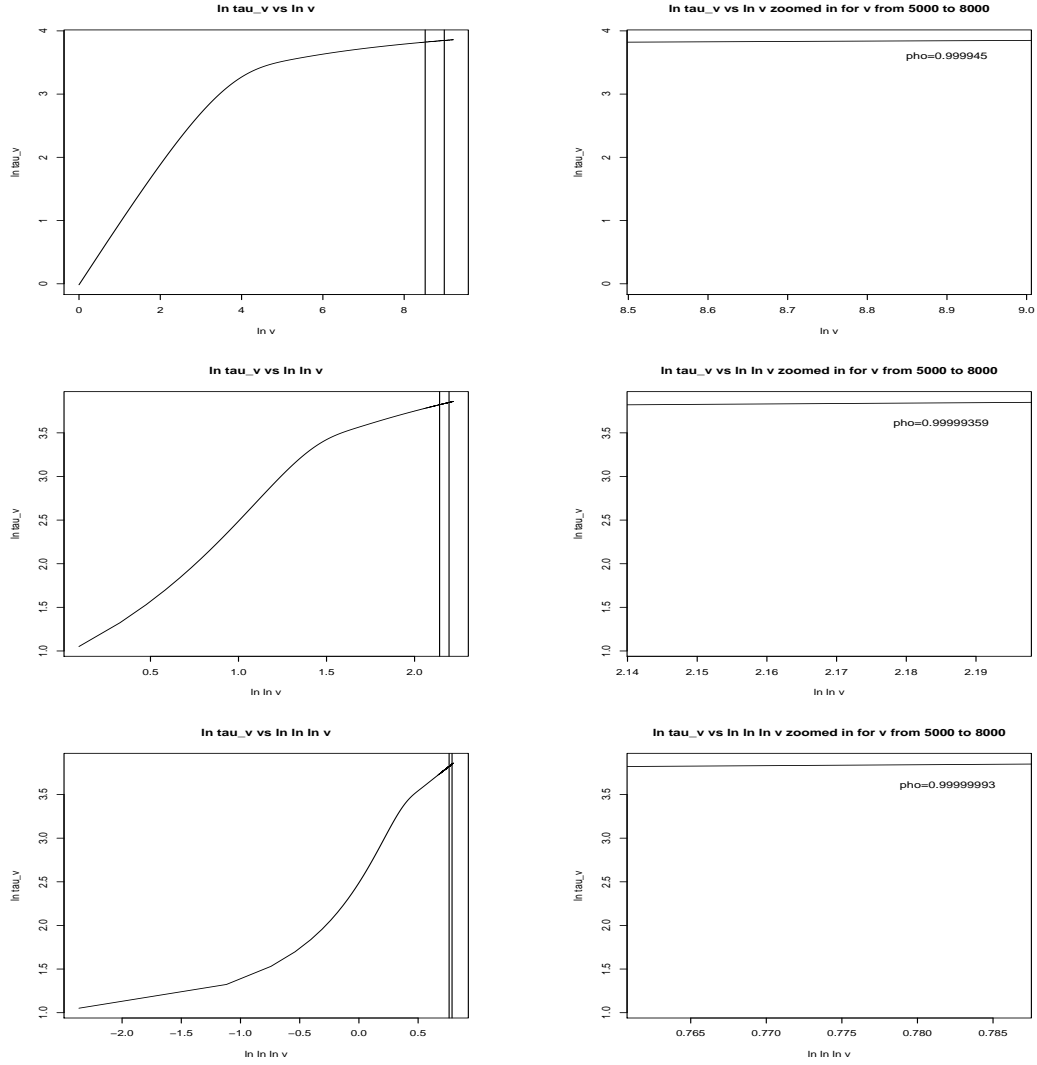


Figure 8: Plots under Distribution 3. Plots on the right side are zoomed for the corresponding part enclosed by two vertical lines on the left-side plots. One observes that although the  $\rho$  in the bottom right plot is the highest, the two  $\rho$ -s on the other right-side plots are also quite close.

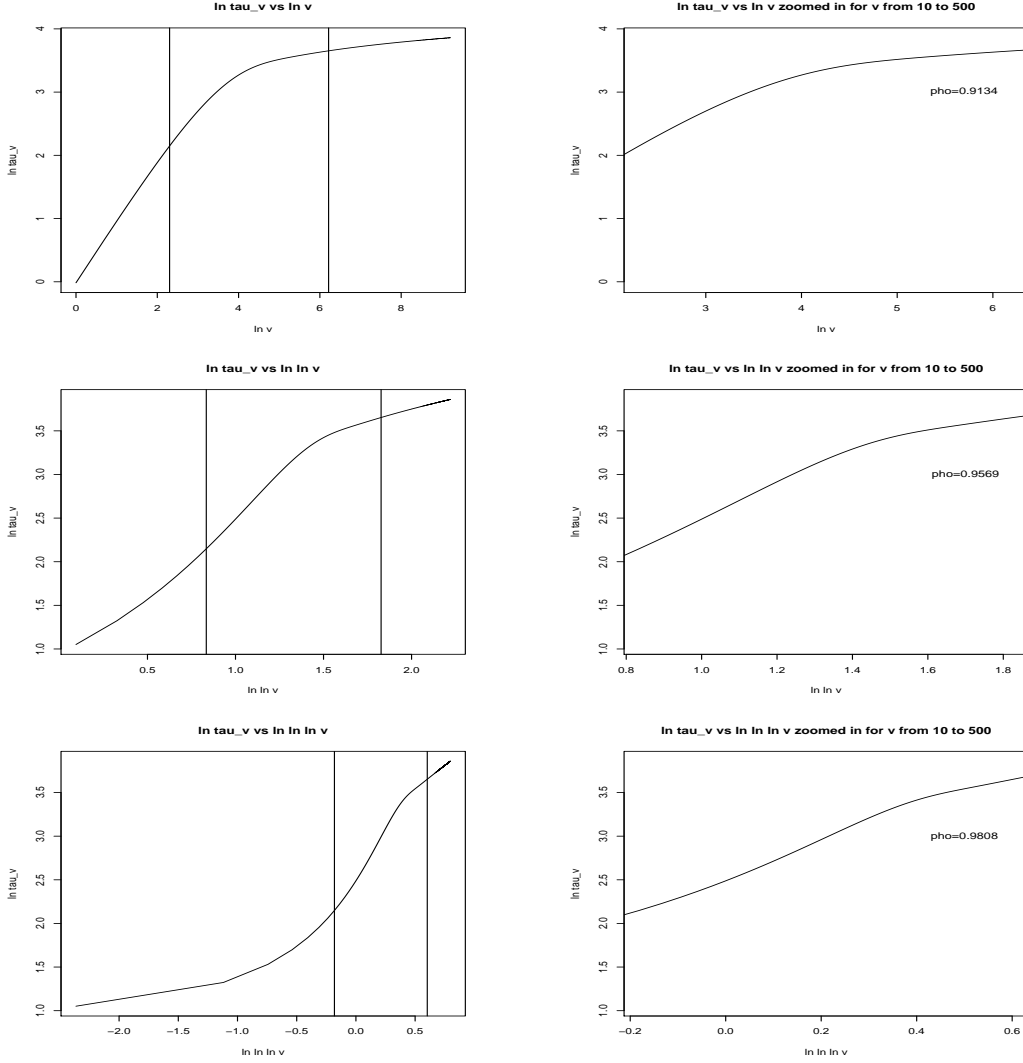


Figure 9: Plots under Distribution 3. Plots on the right side are zoomed for the corresponding part enclosed by two vertical lines on the left-side plots. One observes that although the  $\rho$  in the bottom right plot not as high as the corresponding  $\rho$  in Figure 8, its advantages over the two  $\rho$ -s on the other right-side plots are much larger compare to that in Figure 8.

Second, larger  $v$ -s increase the relative variance of  $T_v$ , because  $T_v$  is established by a U-statistic construction (see Zhang & Zhou (2010)). The larger the  $v$ , the less the sub-samples available, hence a larger relative variance.

Third, a tail profile can be unbiasedly estimated up to  $n - 1$  only.

**Remark 2.** *When selecting the tail profile, a rule of thumb is to select  $v$ -s up to 500*

however large the sample size is.

**Remark 3.** *Regardless of the choice of  $v$ -s, the tail profile always focuses on the type of distribution at the very distance tail, but not at the early stage nor midstream.*

Note that the tail profile at the very beginning should not be used because a larger  $v$  is needed for convergence. If a distribution has vastly different behavior in the tail from the high-frequency region, a larger sample size and  $v$ -s are preferred accordingly. In the simulation study, the tail profile was chosen from  $v = 6$  to  $n/20$  except when the sample size was too small. Besides, for the AMZN example in Section 2, the tail profile was chosen between the 10 and 500, where  $n$  was 30000.

## 5 Proofs

The main theoretical justification for the proposed classifier comes from Proposition 1 and the divergence rates of  $\tau_v$  in (12), (13) and (14) for the three tonic distributional forms of (9), (10) and (11) respectively. To prove Proposition 1, Lemma 1 below is needed. Lemma 1 is a re-statement of Lemma 1.3 of Zhang (2016) where a proof can be found.

**Lemma 1.** *Suppose  $\mathbf{p} = \{p_k; k \geq 1\}$  is such that  $p_k > 0$  for infinitely many positive integer values of  $k$ . Then, as  $v \rightarrow \infty$ ,*

$$\frac{\sum_{k \geq 1} p_k^2 (1 - p_k)^v}{\sum_{k \geq 1} p_k (1 - p_k)^v} \rightarrow 0.$$

*Proof of Proposition 1.* Let  $v = n - 1$ . It can be shown that  $T_{n-1} = [(n - 1)/n] \sum_{k \geq 1} 1[Y_k = 1]$ . Since  $E(T_{n-1}/\tau_{n-1}) = 1$ , it suffices to show that  $\text{Var}(T_{n-1}/\tau_{n-1}) \rightarrow 0$  as  $n \rightarrow \infty$ . Toward

that end, consider

$$\begin{aligned}
\text{Var} \left( \sum_{k \geq 1} 1[Y_k = 1] \right) &= \mathbb{E} \left( \sum_{k \geq 1} 1[Y_k = 1] \right)^2 - \left[ n \sum_{k \geq 1} p_k (1 - p_k)^{n-1} \right]^2 \\
&= \mathbb{E} \left( \sum_{k \geq 1} 1[Y_k = 1] + \sum_{i \geq 1, j \geq 1, i \neq j} 1[Y_i = 1] 1[Y_j = 1] \right) - \left[ n \sum_{k \geq 1} p_k (1 - p_k)^{n-1} \right]^2 \\
&= \left[ \sum_{k \geq 1} n p_k (1 - p_k)^{n-1} + n(n-1) \sum_{i \geq 1, j \geq 1, i \neq j} p_i p_j (1 - p_i - p_j)^{n-2} \right] \\
&\quad - \left[ n \sum_{k \geq 1} p_k (1 - p_k)^{n-1} \right]^2 \\
&\leq n \sum_{k \geq 1} p_k (1 - p_k)^{n-1} + n(n-1) \sum_{i \geq 1, j \geq 1} p_i p_j (1 - p_i - p_j)^{n-2} \\
&\quad - \left[ n \sum_{k \geq 1} p_k (1 - p_k)^{n-1} \right]^2 \\
&\leq n \sum_{k \geq 1} p_k (1 - p_k)^{n-1} + n(n-1) \sum_{i \geq 1, j \geq 1} p_i p_j (1 - p_i - p_j + p_i p_j)^{n-2} \\
&\quad - \left[ n \sum_{k \geq 1} p_k (1 - p_k)^{n-1} \right]^2 \\
&= n \sum_{k \geq 1} p_k (1 - p_k)^{n-1} + n(n-1) \sum_{i \geq 1, j \geq 1} p_i p_j (1 - p_i)^{n-2} (1 - p_j)^{n-2} \\
&\quad - \left[ n \sum_{k \geq 1} p_k (1 - p_k)^{n-1} \right]^2 \\
&= n \sum_{k \geq 1} p_k (1 - p_k)^{n-1} + n(n-1) \left[ \sum_{k \geq 1} p_k (1 - p_k)^{n-2} \right]^2 - \left[ n \sum_{k \geq 1} p_k (1 - p_k)^{n-1} \right]^2.
\end{aligned}$$

$$\begin{aligned}
\text{Var}(T_{n-1}/\tau_{n-1}) &= \left(\frac{n-1}{n\tau_{n-1}}\right)^2 \text{Var}\left(\sum_{k \geq 1} 1[Y_k = 1]\right) \\
&= \left[\frac{n-1}{n(n-1) \sum_{k \geq 1} p_k(1-p_k)^{n-1}}\right]^2 \text{Var}\left(\sum_{k \geq 1} 1[Y_k = 1]\right) \\
&\leq \frac{n}{[n \sum_{k \geq 1} p_k(1-p_k)^{n-1}]^2} \sum_{k \geq 1} p_k(1-p_k)^{n-1} \\
&\quad + \frac{n(n-1)}{[n \sum_{k \geq 1} p_k(1-p_k)^{n-1}]^2} \left[\sum_{k \geq 1} p_k(1-p_k)^{n-2}\right]^2 - 1 \\
&= \frac{1}{n \sum_{k \geq 1} p_k(1-p_k)^{n-1}} + \left(\frac{n-1}{n}\right) \left[\frac{\sum_{k \geq 1} p_k(1-p_k)^{n-2}}{\sum_{k \geq 1} p_k(1-p_k)^{n-1}}\right]^2 - 1 \\
&= \frac{1}{n \sum_{k \geq 1} p_k(1-p_k)^{n-1}} \\
&\quad + \left(\frac{n-1}{n}\right) \left[\frac{\sum_{k \geq 1} p_k(1-p_k)^{n-2}}{\sum_{k \geq 1} p_k(1-p_k)^{n-2} - \sum_{k \geq 1} p_k^2(1-p_k)^{n-2}}\right]^2 - 1 \\
&= \frac{1}{n \sum_{k \geq 1} p_k(1-p_k)^{n-1}} + \left(\frac{n-1}{n}\right) \left[\frac{1}{1 - \frac{\sum_{k \geq 1} p_k^2(1-p_k)^{n-2}}{\sum_{k \geq 1} p_k(1-p_k)^{n-2}}}\right]^2 - 1. \tag{15}
\end{aligned}$$

The first term in (15) goes to 0 since  $\tau_{n-1} \rightarrow \infty$ ; the second term in (15) goes to 1 by Lemma 1. It immediately follows that  $\text{Var}(T_{n-1}/\tau_{n-1}) \rightarrow 0$ .

Next, consider the case of  $v = n - r_n$  where  $r_n$  is an integer satisfying  $r_n \leq n - 1$  and  $r_n \rightarrow \infty$  as  $n \rightarrow \infty$ . In this case, an important fact to be noted is that  $T_{n-r_n}$  is a  $U$ -statistic, constructed by Zhang & Zhou (2010). This  $U$ -statistic is based on a kernel function,  $T_{m-1}^{(*)} = [(m-1)/m] \sum_{k \geq 1} 1[Y_k^{(*)} = 1]$  where  $\{Y_k^{(i)}; k \geq 1\}$  is the set of observed letter frequencies in a sample of size  $m = n - r_n + 1$ , and the estimator may be re-expressed as

$$T_{n-r_n} = \binom{n}{n-r_n+1}^{-1} \sum_* T_{m-1}^{(*)},$$

the average of all  $T_{m-1}^{(*)}$ s based on all possible  $\binom{n}{n-r_n+1}$  sub-samples of size  $m$  from the *iid* sample of size  $n$ . Utilizing the inequality,  $\text{Var}((X_1 + X_2)/2) \leq \text{Var}(X_1)$ , for identically distributed (not necessarily independent) random variables  $X_1$  and  $X_2$ , it follows that

$$\text{Var}(T_{n-r_n}) \leq \text{Var}(T_{m-1}^{(j)}) \rightarrow 0$$

where  $j$  indexes any one of  $\binom{n}{n-r_n+1}$  sub-samples of size  $m = n - r_n + 1$ . □

Next, the convergence rates, (12), (13) and (14), are established for the three distributions in (9), (10) and (11) respectively. Toward that end, a general result established by Molchanov et al. (2018) is re-stated below as Lemma 2.

Consider the following five conditions on the underlying distribution  $\mathbf{p} = \{p_k; k \geq 1\}$ .

C1: Assume  $p_{k+1}/p_k \rightarrow 1$ ;

C2: assume there exists a smooth  $C^2(R_+)$  interpolation  $p(x)$  for  $x > 0$  such that  $p_k = p(k)$  for all  $k$ ,  $p(0) < \infty$ , and  $p'(x) < 0$  for  $x \geq x_0$  where  $x_0$  is a sufficiently large number;

C3: assume the underlying interpolation  $p(x)$  satisfies

(a)  $(\ln p(x))' = p'(x)/p(x) \nearrow 0$ , as  $x \rightarrow \infty$  and

(b)  $\lim_{x \rightarrow \infty} p^2(x)/p(x) = 0$ .

C4: assume  $(p'(x)/p(x))' \geq 0$ ; and

C5: assume that there exists a constant  $\gamma \in [0, 1]$ , such that

$$\limsup_{x \rightarrow \infty} \frac{p''(x)p(x) - (p'(x))^2}{(p'(x))^2} = 1 - \gamma.$$

**Lemma 2.** *Under Conditions C1-C5,  $\tau_v \asymp p(x_v)/|p'(x_v)|$  where  $x_v$  is the root of  $vp(x) = 1$ .*

**Proposition 2.** *For a  $\mathbf{p}$  in the form of (9), (10) or (11), the corresponding  $\tau_v$  increases to infinity, as  $v \rightarrow \infty$ , at the rate of (12), (13) or (14) respectively.*

To prove Proposition 2, Lemma 3 below is needed.

**Lemma 3.** *Let  $x_v$  be the root of equation*

$$\frac{x^{1/\beta}}{\ln x} = (\ln v)^{1/\beta} \tag{16}$$

where  $\beta > 0$  is a positive constant. As  $v \rightarrow \infty$ ,  $\ln x_v \asymp \ln \ln v$  and  $x_v \asymp (\ln v)(\ln \ln v)^\beta$ .

Proof. Condition (16) may be re-expressed as

$$x_v^{1/\beta} = (\ln x_v)(\ln v)^{1/\beta}. \quad (17)$$

For sufficiently large  $x_v$ , or equivalently sufficiently large  $v$ ,  $\ln x_v > 1$  and hence  $x_v^{1/\beta} > (\ln v)^{1/\beta}$ , or

$$\ln x_v > \ln \ln v. \quad (18)$$

On the other hand, for sufficiently large  $x_v$ , or equivalently sufficiently large  $v$ ,

$$x_v^{\frac{1}{2\beta}} < \frac{x_v^{\frac{1}{\beta}}}{\ln x_v} = (\ln v)^{1/\beta}$$

and hence

$$\ln x_v < 2 \ln \ln v. \quad (19)$$

It follows from (18) and (19) that

$$\ln \ln v < \ln x_v < 2 \ln \ln v,$$

that is,  $\ln x_v \asymp \ln \ln v$ , or

$$\begin{aligned} (\ln v)^{1/\beta} \ln \ln v &< (\ln x_v)(\ln v)^{1/\beta} < 2(\ln v)^{1/\beta} \ln \ln v, \text{ or} \\ (\ln v)^{1/\beta} \ln \ln v &< x_v^{1/\beta} < 2(\ln v)^{1/\beta} \ln \ln v, \text{ or} \\ (\ln v)(\ln \ln v)^\beta &< x_v < 2^\beta (\ln v)(\ln \ln v)^\beta, \end{aligned}$$

that is,  $x_v \asymp (\ln v)(\ln \ln v)^\beta$ . □

Proof of Proposition 2. For each of the tonic forms in (9), (10) and (11), Molchanov, Zhang and Zheng (2018) showed that Conditions C1-C5 are all satisfied. It only remains to derive the rates of divergence using Lemma 2, that is,  $p(x_v)/|p'(x_v)|$ .

For (9), the root of the equation  $p(x) = cx^{-\lambda} = 1/v$  is  $x_v = (cv)^{1/\lambda}$ , and  $p'(x) = -\lambda cx^{-(1+\lambda)}$ . It follows that  $p(x_v) = 1/v$  and  $p'(x_v) = -\lambda c^{-(1/\lambda)} v^{-(1+1/\lambda)}$  and that  $p(x_v)/|p'(x_v)| = (c^{1/\lambda}/\lambda)v^{1/\lambda}$ .

For (10), the root of the equation  $p(x) = ce^{-\lambda x^\alpha} = 1/v$  is  $x_v = (\ln(cv)/\lambda)^{1/\alpha}$ , and  $p'(x) = -\lambda \alpha c x^{\alpha-1} e^{-\lambda x^\alpha}$ . It follows that  $p(x_v) = 1/v$  and  $p'(x_v) = -\alpha \lambda \ln(cv)^{1-1/\alpha}/v$  and that  $p(x_v)/|p'(x_v)| = \alpha^{-1} \lambda^{-1/\alpha} (\ln c + \ln v)^{1/\alpha-1}$ .



For (11), the root of the equation  $p(x) = ce^{-\lambda x/(\ln x)^\beta} = 1/v$  does not have an analytic form. However, rewriting the equation gives

$$\frac{x^{1/\beta}}{\ln x} = (\ln(cv)^{1/\lambda})^{1/\beta}.$$

Applying Lemma 3, the root of the equation satisfies

$$\ln x_v \asymp \ln \ln ((cv)^{1/\lambda}) = -\ln \lambda + \ln \ln(cv).$$

Noting

$$p'(x) = -p(x)\lambda \frac{(\ln x)^\beta - \beta(\ln x)^{\beta-1}}{(\ln x)^{2\beta}},$$

it follows that

$$\frac{p(x_v)}{|p'(x_v)|} = \frac{(\ln x_v)^{\beta+1}}{\ln x_v - \beta} \sim (\ln x_v)^\beta \asymp (\ln \ln v)^\beta.$$

□

## References

- Chao, A., Lee, S.-M. & Chen, T.-C. (1988), ‘A generalized good’s nonparametric coverage estimator’, *Chinese Journal of Mathematics* pp. 189–199.
- Esty, W. W. et al. (1983), ‘A normal limit law for a nonparametric estimator of the coverage of a random sample’, *The Annals of Statistics* **11**(3), 905–912.
- Good, I. J. (1953), ‘The population frequencies of species and the estimation of population parameters’, *Biometrika* **40**(3-4), 237–264.
- Molchanov, S., Zhang, Z. & Zheng, L. (2018), ‘Entropic moments and domains of attraction on countable alphabets’, *Mathematical Methods of Statistics* **27**(1), 60–70.
- Robbins, H. E. et al. (1968), ‘Estimating the total probability of the unobserved outcomes of an experiment’, *The Annals of Mathematical Statistics* **39**(1), 256–257.
- Zhang, C.-H. & Zhang, Z. (2009), ‘Asymptotic normality of a nonparametric estimator of sample coverage’, *The Annals of Statistics* **37**(5A), 2582–2595.

- Zhang, Z. (2016), *Statistical Implications of Turing's Formula*, John Wiley & Sons.
- Zhang, Z. (2018), 'Domains of attraction on countable alphabets', *Bernoulli* **24**(2), 873–894.
- Zhang, Z. & Huang, H. (2008), 'A sufficient normality condition for turing's formula', *Journal of Nonparametric Statistics* **20**(5), 431–446.
- Zhang, Z. & Zhou, J. (2010), 'Re-parameterization of multinomial distributions and diversity indices', *Journal of Statistical Planning and Inference* **140**(7), 1731–1738.